The Dynamic Behavior of a Concentrated Polymeric Suspension Containing Non-Brownian Glass Fibers in Simple Shear Flow

*Aaron P. R. Eberle[†], Gregorio M. Velez[‡], Donald G. Baird[†], and Peter Wapperom**
[†]Department of Chemical Engineering, [‡]Macromolecules and Interfaces Institute and
**Department of Mathematics, Virginia Polytechnic and State University, Blacksburg, VA*

Abstract

In this paper we study the dynamic behavior of a concentrated short glass fiber suspension subject to simple shear flow. In particular we are interested in determining the relationship between the stress growth functions (shear and first normal stress) and the evolution of the fibers' orientation distribution within the sample. Stress growth experiments, in start-up of flow, are performed on a Rheometrics Mechanical Spectrometer (RMS-800). Samples at rest are deformed at a constant strain rate for a specified time (i.e. strain) that correlates various points of interest on a stress growth vs. strain plot. The sample temperature is then lowered below the suspension melt temperature "freezing" the fiber orientation. The fiber orientation within the sample is characterized using confocal laser microscopy. The experimental results are then compared to predictions based on the generalized Jeffery equation. It is found that the theory predicts the fiber orientation to evolve faster than is seen experimentally.

Introduction

Glass fibers have been used for decades to improve the mechanical, thermal and insulative properties of polymers [1]. These property improvements are highly dependent on the orientation distribution of the glass fiber. This makes it desirable to not only be able to predict the rheological behavior of a composite fluid but the orientation of the fiber generated during processing to maximize the mechanical properties of the final part [2].

The overall goal of our research is to be able to accurately predict the orientation of fibers suspended in polymer melts generated during injection molding using a finite element analysis. In an attempt to minimize the computational effort of the simulation, it is of a primary interest to establish a constitutive equation capable of predicting the average fiber orientation and bulk stresses. To accomplish this goal one must first establish and assess the ability of a constitutive equation to accurately predict the rheology and associated fiber microstructure of a composite fluid in rheometrical flows which has been the topic of many publications [3, 4].

The first theoretical work that is easily extendable to rigid rods (fibers) is the work of Jeffery [6]. Jeffery extended Einstein's approach to solving the equations of motion for the flow of a Newtonian fluid around a spherical particle to that of a neutrally buoyant, non-interacting, ellipsoidal particle in the absence of Brownian motion. The product of Jeffery's analysis is two periodic functions which describe the particles rotation about the azimuthal and zenith angles in spherical coordinates. The equations predict a three dimensional orientation that never reaches a steady state under dynamic conditions termed a Jeffery orbit. Experimentally, Jeffery orbits have been observed in various dilute systems of high aspect ratio particles where inter-particle hydrodynamic effects and contact are negligible.

Current approaches to predicting the rheology and microstructure of concentrated suspensions either directly use or are based on a generalized form of Jeffery's equation combine with equations associated with the bulk extra stresses. Recent attempts by researchers to improve on theoretical predictions for semi-concentrated and concentrated suspensions have focused on the equations governing the extra stress contributions. While the generalized Jeffery equation, describing the evolution of the fiber orientation, has remained relatively unchanged. The goal of this paper is to assess the ability of the generalized Jeffery's equation to accurately describe the evolution of the glass fibers orientation in concentrated suspensions typical of composite fluids.

Theory

Evolution of Fiber Orientation: The most common approach to represent the orientation state of a fiber is by defining a unit vector, $\mathbf{u}$, parallel to the fiber backbone. In the case of an ideal suspension which consists of a large number of fibers that are identical in size and shape and whose concentration is spatially uniform the average orientation state of the fibers can be described with an orientation distribution function, $\Psi(\mathbf{u},t)$ [6]. The most convenient way to describe the average orientation is with the orientation order parameter tensor, $\mathbf{A}$, and is defined as the second moment of the orientation distribution function:

$$\mathbf{A}(t) = \int_{\mathbf{u}} \mathbf{uu}\Psi(\mathbf{u},t)d\mathbf{u} \tag{1}$$

The trace of $\mathbf{A}$ is always equal to 1 and for a completely random orientation A_{11}, A_{22} and A_{33} = 1/3. In the limit where all the fibers are perfectly aligned in the 1-direction, A_{11} = 1.

For simple flows the generalized Jeffery equation can be written in terms of $\mathbf{A}$ as follows with the use of the quadratic closure approximation [6]:

$$\frac{d\mathbf{A}}{dt} = \left(\mathbf{A}\cdot\mathbf{W} - \mathbf{W}\cdot\mathbf{A}\right) + \lambda\left(\mathbf{D}\cdot\mathbf{A} + \mathbf{A}\cdot\mathbf{D} - \mathbf{D}:\mathbf{AA}\right) \quad (2)$$

where $\mathbf{W} = ½*[(\nabla v) - (\nabla v)^t]$, $\mathbf{D} = ½*[(\nabla v) + (\nabla v)^t]$, ∇v is the velocity gradient and λ is a constant defining the ellipticity of the particle. For fibers it is common to assume the particle's aspect ratio approaches infinity in which case $\lambda \rightarrow 1$ and Eq. (2) predicts the period of rotation for the fiber to be infinitely long. In the results and discussion section, predictions using Eq. (2) with $\lambda = 1$ for simple shear flow kinematics are compared to experimental results.

Measurement of Fiber Orientation: To determine the components of **u** for a large number of fibers and establish the average orientation state of the system, images of various samples were taken at cross-sectional planes perpendicular to the flow direction. This procedure is described in detail in the following section, Experimental Procedure. In the images the cross-section of each fiber appears as an ellipse. From the ellipse the zenith angle (θ) is measured directly from the image. The zenith angle is the angle measured from the z or 3-axis to a line drawn through the major axis of the ellipse. To clarify this procedure, a schematic representation of a fiber cross-section is shown in Fig. 1 (a) with the zenith angle directly determine from the image. The azimuthal angle (ϕ), illustrated in Fig. 1(b), is determined from the magnitude of the major, M, and minor axis, m, of the ellipse as follows:

$$\left|\cos\phi\right| = \frac{m}{M}, \quad 0 \le \phi \le 90^o \quad (3)$$

The limitation of calculating ϕ with Eq. (3) is the solution is always the positive root. Hence one does not know if the correct angle is ϕ or the fiber's mirror image $90^o + \phi$. For these geometric equations to be valid it is assumed that the fibers are perfectly rigid circular cylinders [7].

To increase the accuracy of the 3D description of fiber orientation, described above, images were taken using a confocal laser microscope. This allowed for images to be taken at multiple planes within the sample and, theoretically, fully describe the 3D fiber orientation without the ambiguity of determining ϕ from just one plane. To clarify this technique Fig. 2 illustrates two fibers whose orientation is the mirror image of each other and are bisected by two planes. When only one plane is analyzed it is impossible to distinguish the difference in orientation between the two fibers. However, when images from two planes are overlapped the centers of mass of the two ellipses move in different directions. This allows for the correct angle ϕ to be determined.

After processing the images relating to the experimental data, it was found that change in center of mass for the two superimposed planes was only possible when the aspect ratio of the ellipse was greater than three. For this reason we term our analysis "pseudo-3D" in that there is still a certain amount of ambiguity with the ϕ-angle for fibers who were mostly aligned in the 1-direction. The other error associated with this technique, assuming the fibers are rigid, is a result of determining the exact size and orientation of the ellipse from the digital images.

With the θ and ϕ angles the components of the vector **u** can be determined for each fiber. The tensor **A** is then determined as follows:

$$A_{ij} = \frac{\sum\left(u_i u_j\right)F_n}{\sum F_n}, \ldots F_n = \frac{M_n}{m_n} \quad (4)$$

where F_n is a weighting function for the nth fiber. The weighting function is based on the probability of bisecting a fiber. Meaning, a fiber aligned perpendicular to the plane of bisection is more likely to be bisected than one aligned parallel. Using the weighting function, the larger the aspect ratio of the ellipse, the more that fiber is weighted.

Experimental Procedure

Rheology: All experiments were performed on a 30 wt% short glass fiber-filled polybutylene terephthalate (PBT). The neat PBT suspending medium exhibited little shear thinning behavior: 420 Pa*s @ 0.1 rad/s, 320 Pa*s @ 100 rad/s. Hence, the suspending medium behaved similarly to a Newtonian fluid. The suspension's specifications can be found in Table 1. All rheological measurements were performed on a Rheometrics Mechanical Spectrometer (RMS-800) fitted with 50 mm diameter cone and plate geometry to ensure a homogeneous shear field within the rheometer gap. All samples were dried at 120 ^{o}C for a minimum of four hours in a vacuum oven at a pressure of 0.3 (in.Hg) before sample molding or testing.

To minimize the degree of boundary interaction, it has been suggested that the rheometer gap be at least three times the length of the longest dimension of the suspension particle [8]. Experimental results using parallel plate geometry with various rheometer gaps confirmed that for the 30 wt% glass fiber-filled PBT there is a negligible effect on the sample rheological response when the gap is greater than twice the number average fiber length. The gap within the 50 mm cone and plate fixture varies linearly from 2.51 mm at the outer edge to 0.05 mm at the center. To remove the inevitable fiber-boundary interaction near the center, sample disks were pre-formed and a 25.4 mm diameter hole was drilled through the center creating a donut shaped sample. A schematic of the "donut" sample can be seen in Fig. 3. This insured that that gap was always greater than two times the number average fiber length.

Confocal Laser Microscopy: To characterize the evolving fiber orientation under dynamic conditions,

donut samples composed of the 30 wt% PBT were deformed using the RMS-800 with the cone and plate geometry at a shear rate of 1 s^{-1} for a specified amount of time at 260 ^{o}C in a nitrogen environment. After which the sample temperature was immediately lowered below the suspension melt temperature, "freezing" the flow induced fiber orientation. The samples were then bisected at the center of the sample creating a plane perpendicular to the flow direction. The samples were then encapsulated in epoxy and the bisection plane was sanded and polished to a final abrasive particle size of 0.3 μm Al_2O_3. Images of the polished surface were taken using a Zeiss LSM510 confocal laser scanning microscope fitted with a 40x water immersion objective lens and a laser excitation wavelength of 543 nm. The confocal laser is able to focus on the sample surface and penetrate the sample to a depth of 10 μm. For each sample ten sequential images were taken from the bottom of the donut sample to the top at a position of 22 mm from the center. An illustration of depicting the position at which the pictures were taken can be seen in Fig. 3. The cross-section of each fiber appeared as a circle or ellipse. To process the image, the circumference of each ellipse was traced by hand in power point to improve the contrast between the fibers and the matrix. Figures 4 (a) and (b) depict images acquired with the confocal laser microscope and the image with ellipses drawn around the fiber cross-sections respectively. The image was then converted to a binary, black and white, image. A simple computer program was written combined with image analysis software in Matlab that measured the position of center of mass, the major and minor axis and θ angle of each ellipse. For each sample the total number of ellipses analyzed varied from 321 for strain = 4 to roughly 456 for strain = 200.

Model: The generalized Jeffery equation, Eq. (2), was solved numerically for simple shear flow kinematics ($v_1 = \dot{\gamma} y$ and $v_2 = v_3 = 0$) with $\lambda = 1$. Gears implicit predictor-corrector method for stiff differential equations was used to solve the coupled equations at a time step of 0.01 s. The initial conditions were taken from those found experimentally and can be found in Tables 1 and 2 relating to strain = 0.

Results and Discussion

The transient rheological behavior of the 30 wt% short glass fiber-filled PBT in start-up of simple shear flow can be summarized with Fig. 5. Figure 5 depicts the shear stress and first normal stress difference vs. strain in an interrupted start-up of flow experiment for a donut sample. The initial fiber orientation of the sample is discussed in detail subsequently, but is mostly oriented in the 1 and 3 directions (defined in Fig. 3). During start-up of flow the stresses, both shear and first normal stress difference (N_1), exhibit large stress overshoots. The overshoot in the shear stress reaches a steady state in roughly 50 strain units while the overshoot in N_1 takes roughly 75 strain units to reach a steady state. The overshoot in the stresses are believed to be a result of the rods rotating to align themselves in the flow direction. After 100 s the flow was stopped and the stresses relax almost instantly, < 2 s. When the flow is re-applied in the same direction the stresses immediately rise to the steady state value and do not exhibit the large overshoots exhibited by a fresh sample. This is a typical result response of non-Brownian particles in which particle sedimentation is negligible. The fact that the overshoot did not reappear after the stresses were allowed to relax is believed to be a result of the rods maintaining their orientation during the stress relaxation. Hence, when the flow is reapplied the stresses immediately grow to their previous value because the rod orientation has not changed.

In an attempt to experimentally characterize the evolving fiber orientation, numerous samples were analyzed at certain points of interest relating to the shear stress and N_1 overshoot, the initial orientation and steady state. The donut samples were all prepared in the same manner and deformed with the cone and plate geometry to specific strain units. In total six samples were analyzed relating to strains of 0, 4, 7, 9, 12 and 200. Strains 0 and 200 related to the initial and steady state orientation of the system respectively. Strains 7 and 9 related to the shear stress and N_1 overshoot peaks respectively and strains 4 and 12 where intermediate points. Tables 2 and 3 summarize the average orientation state of the samples at each strain.

The experimental results for the fiber orientation suggests that the majority of the fibers are initial oriented in the 1 and 3-directions with little orientation in the 2-direction. This can be seen in Table 2, the diagonal components of **A**, for strain = 0, $A_{11} = 0.424$, $A_{22} = 0.170$ and $A_{33} = 0.406$. Upon start-up of flow, tracking the **A** components with increasing strain, the A_{11} component decrease before increasing again while almost simultaneously the A_{33} component increases before decreasing. The A_{22} exponentially decreases immediately. These results suggest that few if any fibers exhibit end-over-end tumbling in the 1-2 plane, but there does seem to be a high rotation of fibers in the 1-3 plane.

The experimental results are compared to model predictions based on the generalized Jeffery's equation. The results are also summarized in Tables 1 and 2 termed **TA**. In addition, the diagonal components are graphed and compared to the model predictions in Fig. 6. Jeffery's equation predicts that within 7 strain units the fibers are almost fully aligned in the flow direction ($TA_{11} = 0.949$ @ strain = 7) while experimental data shows that at a strain of 12, $A_{11} = 0.621$. Hence the fibers are not nearly as aligned as the model predicts. We speculate that this must be due to direct inter-particle interaction hindering the fiber rotation. At a strain of 200 the model predicts that the fibers are completely aligned, $TA_{11} = 0.999$. The experimental data does show that the fibers are aligning themselves in the flow direction, $A_{11} = 0.858$, just not as quickly as the model would suggest. It is

unclear if the fiber orientation every reaches a steady state due to the lack of experimental data at the intermediate strains.

Lastly, we would like to discuss the evolution of the A_{12} component. Rheological theories for fiber suspensions in Newtonian fluids indicate that large shear stress values arise when the fiber orientation has a component in A_{12} [3]. This has led authors to assume that the stresses are primarily a result of fiber rotation. Experimentally, the A_{12} component never exhibits a significant increase over the initial value. However the model predicts an increase that then decreases to a steady state, similar to a stress overshoot. This behavior can be seen in Fig. 7 where the experimental data is compared to the theoretical predictions, A_{12} and TA_{12} respectively. The experimental data implies that the large shear stress overshoot exhibited by concentrated suspensions is not a result of the evolving fiber orientation in A_{12}. If this is correct, the large stress overshoots must be a result of direct fiber contact.

Conclusion

Experimentally determined fiber orientation was compared to predictions based on the generalized Jeffery's equation for evolving fiber orientation in simple shear flow. It was found that the theory predicted the fiber orientation to evolve and align in the flow direction much faster than was determined experimentally. In addition, experimental results suggest that the shear stress overshoot is not a result of the A_{12} component of **A**, but direct fiber contact.

Acknowledgements

This work is funded by NSF under Award Number DMI-0521918.

References

1. L. A. Carlson, Thermoplastic Composite Materials: Composite Materials Series, Vol 7, *Elsevier*, New York, (1991).
2. S. Tseng and T. A. Osswald, *Poly. Comp.*, **15**, 270 (1994).
3. S. M. Dinh and R. C. Armstrong, *J. Rheology*, **28**, 207, (1984).
4. M. Sepehr, P. J. Carreau, M. Grmela, G. Ausias, and P. G. Lafleur, *J. Poly. Eng.*, **24**, 579, (2004).
5. Jeffery, G. B., The motion of ellipsoidal particles immersed in a viscous fluid, *Proc R Soc Lond A*, 102, 161-179, (1922).
6. F. P. Folgar and C. L. Tucker, *J. Rein. Plast. Comp.*, **3**, 98, (1984).
7. Y. H. Lee, S. W. Lee, J. R. Youn, K. Chung, and T. J. Kang, *Mat. Res. Innovat.*, **6**, 65, (2004).
8. W. R. Blankeney, *J. Colloid Interface Sci.*, **22**, 324, (1966).

Table 1. Suspension specifications.

PBT Density (g/cm^3)	Wt %	Vol %	L_n	L_w	a_r
1.31	30	17.66	0.36	0.44	30

Table 2. Experimental, **A**, and predicted (using the generalized Jeffery), **TA**, diagonal components of the orientation order parameter tensor.

Strain	A_{11}	TA_{11}	A_{22}	TA_{22}	A_{33}	TA_{33}
0	0.424	0.424	0.170	0.170	0.406	0.406
4	0.135	0.882	0.105	0.035	0.760	0.083
7	0.504	0.949	0.045	0.015	0.451	0.036
9	0.496	0.967	0.051	0.010	0.453	0.023
12	0.621	0.980	0.056	0.006	0.323	0.014
200	0.858	0.999	0.056	0.000	0.086	0.000

Table 3. Experimental, **A**, and predicted (using the generalized Jeffery), **TA**, off-diagonal components of the orientation order parameter tensor.

Strain	A_{12}	TA_{12}	A_{13}	TA_{13}	A_{23}	TA_{23}
0	0.143	0.143	0.291	0.291	0.164	0.164
4	0.084	0.081	0.254	0.195	0.218	0.017
7	0.059	0.052	0.283	0.126	0.080	0.007
9	0.071	0.041	0.294	0.101	0.095	0.004
12	0.132	0.032	0.251	0.078	0.072	0.002
200	0.142	0.005	0.192	0.005	0.048	0.000

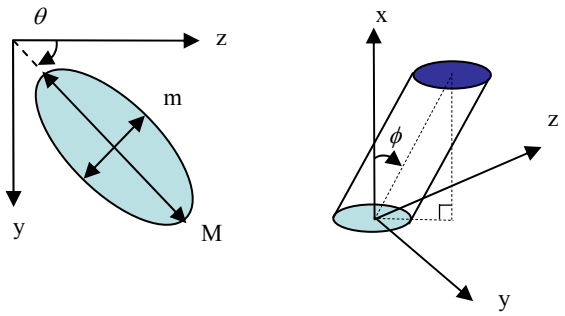

Figure 1. (a) Elliptical "footprint" of fiber cross-section. Zenith angle is determined by direct measurement from the z-axis. (b) Illustration defining azimuthal angle in rectilinear coordinates [8].

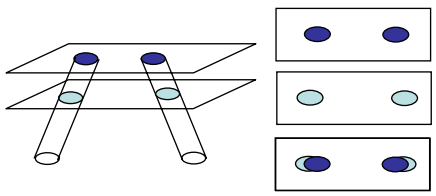

Figure 2. Two fibers whose orientations are the mirror image of one another that are bisected by two planes.

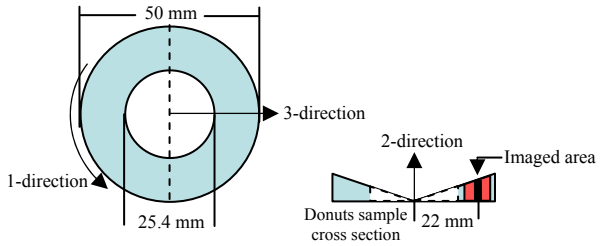

Figure 3. 50 mm cone and plate "donut sample" dimensions. The illustration defines the 1, 2, and 3-directions which are the direction of flow, velocity gradient and radial directions respectively. In the cross-sectional profile the black area is the area at which the confocal laser images were taken.

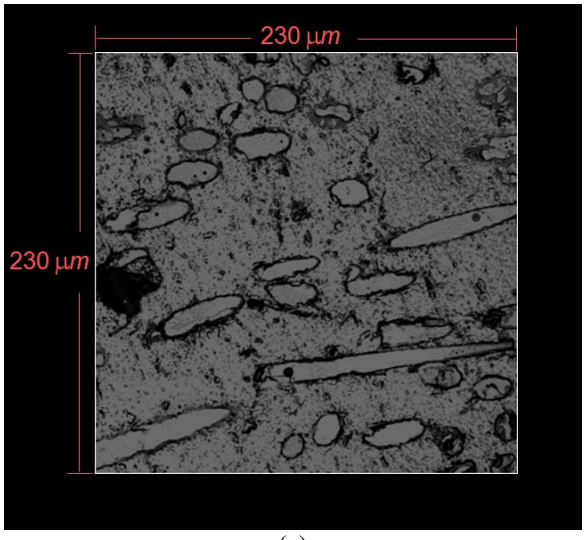

(a)

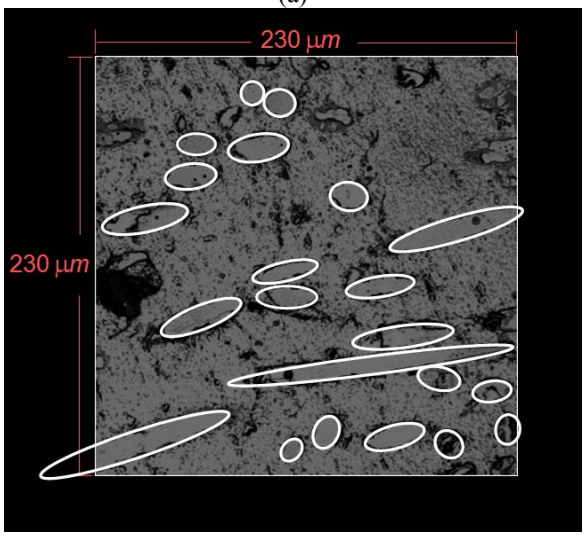

(b)

Figure 4. Confocal laser image of the 30 wt% PBT sample. The circles and ellipses are the cross-section of glass fibers within the sample. (a) Raw image. (b) Processed image, ellipses were drawn around each fiber to increase the contrast with the matrix.

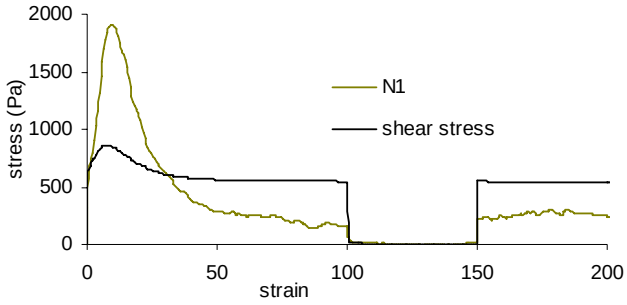

Figure 5. Shear stress and first normal stress difference vs. strain in an interrupted start-up of flow experiment for a 30 wt% short glass fiber-filled PBT. Test conditions: shear rate = 1 s^{-1}, temperature = 260 ^{o}C, and nitrogen environment.

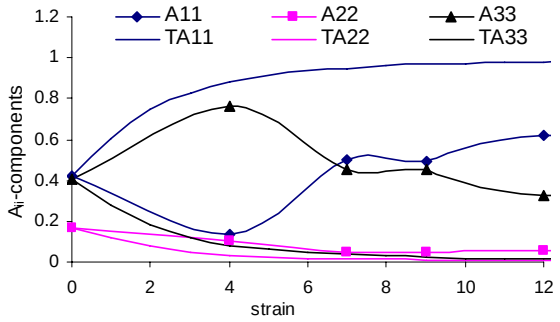

Figure 6. Shear stress and first normal stress difference vs. strain in an interrupted start-up of flow experiment for a 30 wt% short glass fiber-filled PBT. Test conditions: shear rate = 1 s^{-1}, temperature = 260 ^{o}C, and nitrogen environment.

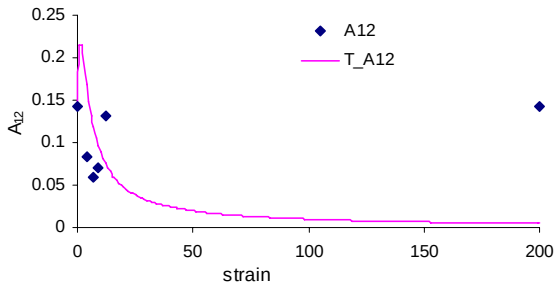

Figure 7. Evolution of the 1,2-compent of the orientation order parameter tensor. Experimental A, and theoretical TA.

Key Words: glass fiber, suspension, orientation, rheology, confocal laser microscopy